The Cryosphere Discuss., https://doi.org/10.5194/tc-2017-188
Manuscript under review for journal The Cryosphere
Discussion started: 22 September 2017

Relative performance of empirical and physical models in assessing seasonal and annual glacier surface mass balance in the French Alps

Marion REVEILLET[1*], Delphine SIX[1], Christian VINCENT[1], Antoine RABATEL[1], Marie DUMONT[2], Matthieu LAFAYSSE[2], Samuel MORIN[2], Vincent VIONNET[2] and Maxime LITT[3-1].

[1] Univ. Grenoble Alpes, CNRS, IRD, Institut des Géosciences de l'Environnement (IGE, UMR 5001), F-38000 Grenoble, France

[2]Météo-France CNRS, CNRM/CEN UMR 3589, Météo-France, CNRS, Grenoble, France

[3] ICIMOD, GPO Box 3226, Kathmandu, Nepal

[*] now at: Centro de Estudios Avanzados en Zonas Áridas (CEAZA), ULS-Campus Andrés Bello, Raúl Britan 1305, La Serena, Chile

Correspondence to: Marion REVEILLET (marion.reveillet@ceaza.cl)

Abstract. This study focuses on simulations of the seasonal and annual surface mass balance (SMB) of Saint-Sorlin Glacier (French Alps) for the period 1996-2015 using the detailed SURFEX/ISBA-Crocus snowpack model. The model is forced by SAFRAN meteorological reanalysis data, adjusted with AWS measurements to ensure that simulations of all the energy balance components, in particular turbulent fluxes, are accurately represented with respect to the measured energy balance. Results indicate good model performance for the simulation of summer SMB when using meteorological forcing adjusted with in-situ measurements. Model performance however strongly decreases without in-situ meteorological measurements. The sensitivity of the model to meteorological forcing indicates a strong sensitivity to wind speed, higher than the sensitivity to ice albedo. Compared to an empirical approach, the model exhibited better performance for simulations of snow and firn melting in the accumulation area and similar performance in the ablation area when forced with meteorological data adjusted with nearby AWS measurements. When such measurements were not available close to the glacier, the empirical model performed better. Our results suggest that simulations of the evolution of mass balance in the future using energy balance model required very accurate meteorological data which are not reliable from the climatic scenarios. With the current status of knowledge on meteorological variables and glacier surface roughness in the future, empirical approaches based on temperature and precipitation could be more appropriate for simulations of glaciers in the future.

The Cryosphere Discuss., https://doi.org/10.5194/tc-2017-188
Manuscript under review for journal The Cryosphere
Discussion started: 22 September 2017

1. Introduction

The surface mass balance (SMB) of mountain glaciers is sensitive to climate change and contributes to the hydrological regime of high alpine catchments (IPCC, 2013). Understanding the physical processes that link local meteorology to glacier melt is necessary to properly simulate changes in glacier SMB in the context of global warming.

Several studies have successfully used various calibrated temperature-index models (TIM) to simulate glacier melt response to meteorological forcing (Braithwaite and Olesen, 1989; Hock, 2003; Pellicciotti *et al.*, 2005). These approaches can be used over short time periods (typically a few years), but the relevance of the calibrated parameters over longer time periods is difficult to assess for several reasons including: (i) the lack of long term *in-situ* meteorological measurements available close to the study site, (ii) the temporal variations of melt sensitivity to temperature and (iii) the fact that the physical link between temperature and melt is not direct (Huss *et al.*, 2009; Gabbi *et al.*, 2014; Réveillet *et al.*, 2017).

On the other hand, physical approaches consider all energy exchanges between the glacier and the atmosphere and are able to represent snow melt spatial and temporal variability, such as those related to albedo variations that are hard to represent in TIM models. Such approaches offer higher transferability over time (e.g., MacDougall and Flowers, 2011) but require more accurate meteorological forcing (e.g., Gabbi *et al.*, 2014). Many energy balance studies have been performed to assess surface-atmosphere interactions over ice or snow surfaces based on automatic weather stations (AWS) deployed on glaciers (e.g., Oerlemans and Klok, 2002; Sicart *et al.*, 2008; Senese *et al.*, 2012; Cullen and Conway, 2015). Physically based models perform well for SMB simulations when AWS measurements are available on the study site (e.g., Six *et al., 2009)* and enable a quantification of each component of the energy budget and their impact on melting. However, due to the need for accurate meteorological data and the difficulty of maintaining AWSs on glaciers, this approach is generally used over short time periods (typically a few months), except for a few studies based on permanent AWSs set up on glaciers (e.g., Oerlemans *et al.*, 2009; Sicart *et al.*, 2011).

These physical models, using *in-situ* meteorological data or coupled with atmospheric models (e.g., Lefebre, 2003; Mölg and Kaser, 2011) or forced by meteorological reanalysis (e.g., Gerbaux *et al.*, 2005), provide an opportunity to determine the spatial distribution of SMB evolution over longer periods. The simulation of seasonal SMB changes requires accurate modelling of energy exchanges over both ice and snow surfaces. Detailed snowpack models such as Crocus (Brun *et al.*, 1989), SNOWPACK (Lehning *et al.*, 1999) or Snow-SVAT (Tribbeck *et al.*, 2004) have been developed and some have been applied to glaciers (e.g., Obleitner and Lehning, 2004; Gerbaux *et al.*, 2005; Dumont *et al.*, 2012; Lejeune *et al.*, 2013; Sauter and Obleitner, 2015). Due to the lack of measurements and the complexity of measuring each of the components of the energy balance (especially turbulent fluxes), physically based models are generally calibrated by adjusting certain parameters (e.g., roughness length to quantify turbulent fluxes) to fit with SMB measurements rather than evaluated using each component of the energy balance.

The goal of our study is to evaluate the performance of a physical model in simulating seasonal SMB and to compare its performance and the associated uncertainties to those obtained with a temperature-index model in order to determine the

most appropriate approach for SMB simulations, especially for projections over long time periods. In the Alps, the temporal variability of the annual SMB is mainly driven by summer SMB variability (e.g., Six and Vincent, 2014). For this reason, many studies have focused on ablation modelling. However, the uncertainties in the simulation of summer SMB strongly depend on the winter SMB (Réveillet *et al.*, 2017), highlighting the need for a quantification of the sensitivity of annual SMB to both seasonal components.

For these purposes, we use the detailed SURFEX/ISBA-Crocus snowpack model (Vionnet *et al.*, 2012), driven by SAFRAN meteorological reanalysis data (Durand *et al.*, 2009), to simulate the SMB of Saint-Sorlin Glacier (French Alps). We first assess the accuracy of SAFRAN meteorological reanalysis data at this high elevation site using all available glaciological and meteorological measurements performed since 2005 on Saint-Sorlin Glacier. Then, the surface energy and mass balance model is calibrated using the measured energy balance to ensure that all the energy balance components are accurately represented. Next, the SMB model is evaluated using twenty years of seasonal SMB measurements (section 4.1.1) and results are compared to those obtained with temperature-index models (section 4.1.2). Section 4.1.3 focuses on annual SMB sensitivity to seasonal SMB. Finally, Crocus model sensitivity to meteorological forcing, calibration and topographic parameters is analysed in section 4.2.

2. Study site and data

2.1 Study site: Saint-Sorlin Glacier

Saint-Sorlin Glacier is located in the Grandes Rousses massif in the French Alps (Figure 1) and is monitored by the GLACIOCLIM program (https://glacioclim.osug.fr). Saint-Sorlin Glacier covers a surface area of roughly 2.5 km^2. The glacier flows along slopes with highly variable aspects, descending from 3460 to 2700 m a.s.l. More details on the topographic characteristics of this glacier are provided in Six and Vincent (2014).

2.2 Glaciological measurements over the period 1995-2015

2.2.1 Seasonal surface mass balance measurements

Seasonal SMB has been monitored since 1995 using the glaciological method (Cuffey and Paterson, 2010) at about 30 measurements points (Figure 1). During summer (*i.e.* from around 15 April to 15 October, corresponding to the ablation season), the glacier is regularly visited and monthly ablation measurements are available. The uncertainties of the SMB measurements are evaluated at approximately ±0.20 m w.e. yr^{-1} for winter surface mass balance (WSMB) and ±0.15 w.e. yr^{-1} (resp. 0.30) for summer surface mass balance (SSMB) on ice (resp. snow/firn) (Thibert *et al.*, 2008). The monitoring network covers a large part of the glacier both in the accumulation and ablation areas (Figure 1). WSMBs are measured at each point located in the accumulation and ablation areas in late April using snow cores and density measurements. SSMBs are quantified using stakes inserted in the ice/snow.

The Cryosphere Discuss., https://doi.org/10.5194/tc-2017-188
Manuscript under review for journal The Cryosphere
Discussion started: 22 September 2017

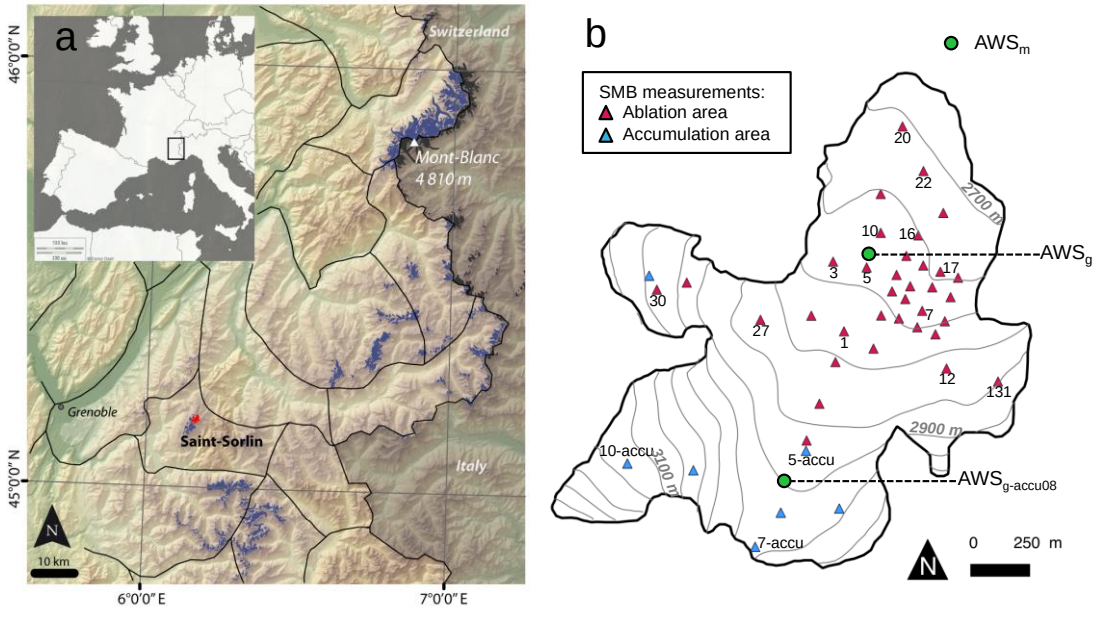

Figure 1. (a) Location of Saint-Sorlin Glacier in the French Alps. French glaciers are shown in blue except for Saint-Sorlin Glacier, used for the present study, which is in red. Black lines represent SAFRAN massif outlines (adapted from Rabatel et al., 2016). (b) Map of Saint-Sorlin Glacier with the network of in-situ SMB measurements (blue triangles in the accumulation area and red triangles in the ablation area). Locations of automatic weather stations used in this study are represented by green circles.

2.2.2 Digital Elevation Models

We used three digital elevation models (DEMs) (1998, 2007 and 2014) to account for the changes in glacier geometry during the studied period. These DEMs were derived from aerial photogrammetry and have a 10-m spatial resolution. For consistency with the resolution of the atmospheric data described in section 2.3.3, they were upscaled to 200-m resolution using a kriging method.

2.3 Meteorological data

2.3.1 Automatic weather stations

In the framework of GLACIOCLIM, a permanent AWS has been in operation since August 2005 on the foreland of Saint-Sorlin Glacier (noted AWS$_m$ on Figure 1b). This AWS records 2-m air temperature (the sensor is housed in a mechanically aspirated shield), relative humidity, short and long-wave radiation and wind speed and direction with a half-hour time step. Data were quality checked to avoid any problem related to a sensor malfunction. An additional meteorological station (noted

AWS_g in Figure 1b) was set up in the ablation area of the glacier during each of the three summer field campaigns (2006, 2008 and 2009). It will be referred to hereafter as AWS_{g06}, AWG_{g08} and AWS_{g09} to distinguish between the different years. Note that during the 2008 field campaign, another AWS was set up in the accumulation area (noted $AWS_{g\text{-}accu08}$ in Figure 1b). Details relative to these AWSs are reported in Table 1.

2.3.2 Eddy covariance system and atmospheric mast

In 2006, a summer field campaign was also conducted to measure turbulent fluxes using the Eddy covariance (EC) method (Table 1). During this campaign (9 July to 28 August 2006), an Eddy covariance system measuring the high frequency (20 Hz) wind speed components, sonic temperature and specific humidity was fixed on a mast in the ablation zone next to AWS_{g06}. Due to ice melt, the instruments were lowered manually every 10 to 15 days. More details on the sensors, the field campaign and data processing are available in Litt *et al.* (2016).

2.3.3 Raw SAFRAN reanalysis data

Since AWS records on glaciers are limited in time and scarcely distributed, the near surface meteorological forcing data are estimated by meteorological reanalyses. In this study, we used the SAFRAN meteorological re-analysis system (Durand *et al.*, 2009). SAFRAN data are provided using atmospheric vertical profiles simulated by an atmospheric model (ERA-40 reanalysis until 2001 and ARPEGE operational model after 2002). Results are then corrected by optimal interpolation with observed meteorological data from various sources (automatic weather stations, manual observations carried out in the climatological network or at ski resorts, remotely-sensed cloudiness, atmospheric upper-level sounding). Note that surface observations that could be used to correct data are scarce at very high altitudes (*i.e.* above 2000 m a.s.l.).

SAFRAN outputs include hourly meteorological variables (2-m air temperature and relative humidity, precipitation amounts and phases, incoming direct and diffuse shortwave radiation, incoming longwave radiation, wind speed, cloudiness) that are assumed to be homogeneous within a given massif (in particular within the Grandes Rousses massif where the Saint-Sorlin Glacier is located, Figure 1a) and depend only on altitude and aspect. The direct solar radiation is provided for an infinite flat area but can be easily projected for any aspect and slope (Lafaysse *et al.*, 2011) using the Crocus model (see section 3.1.1). Shading from surrounding topography is taken into account in the computation of shortwave radiation, but the impact of long and short wave radiation emitted by surrounding slopes is not considered.

SAFRAN outputs are available in 300-m elevation steps. In our study, they were linearly interpolated (following the vertical and horizontal axes) on the 200-m horizontal resolution grid encompassing the glacier.

The Cryosphere Discuss., https://doi.org/10.5194/tc-2017-188
Manuscript under review for journal The Cryosphere
Discussion started: 22 September 2017

Station	Location	Date of records	Timestep	Variables	Instrument	Manufacturer accuracy	Associated studies
AWS_m	Moraine 2720 m a.s.l.	2005-present	30 min	Aspirated air T (°C)	Vaisala HMP45C	±0.2°C	*Six et al.* (2009)
				Relative humidity (%)	Vaisala HMP45C	3%	
				Wind speed (m s^{-1})	Young 05103	0.3 m s^{-1}	*Sicart et al.* (2008)
				and direction (degrees)	Young 05103	±3°	
				Upward SW (W m^{-2})	Kipp and Zonen CG3	0.4%	*Dumont et al.* (2012)
				Downward LW (W m^{-2})			
AWS_{g06}	Ablation area 2770 m a.s.l.	9 July - 28 August 2006	30 min	Aspirated air T (°C)	Vaisala HMP45C	±0.2°C	*Dumont et al.* (2012)
				Relative humidity (%)	Vaisala HMP45C	3%	
				Wind speed (m s^{-1})	Young 05103	0.3 m s^{-1}	
				and direction (degrees)	Young 05103	±3°	*Litt et al.* (2016)
				Upward SW (W m^{-2})	Kipp and Zonen CG3	0.4%	
				Downward LW (W m^{-2})	Csat3 and Licor 7500	0.4%	
$AWS_{g-accu08}$	Accumulation area 2900 m a.s.l.	12 July - 10 September 2008	30 min	EC measurements			
				Aspirated air T (°C)	Vaisala HMP45C	±0.2°C	*Dumont et al.* (2012)
				Relative humidity (%)	Vaisala HMP45C	3%	
				Wind speed (m s^{-1})	Young 05103	0.3 m s^{-1}	
				and direction (degrees)	Young 05103	±3°	
				Upward SW (W m^{-2})	Kipp and Zonen CG3	0.4%	
				Downward LW(W m^{-2})			
AWS_{g08}	Ablation area 2770 m a.s.l.	11 July - 2 August 2008	30 min	Aspirated air T (°C)	Vaisala HMP45C	±0.2°C	*Dumont et al.* (2012)
				Relative humidity (%)	Vaisala HMP45C	3%	
				Wind speed (m s^{-1})	Young 05103	0.3 m s^{-1}	
				and direction (degrees)	Young 05103	±3°	
				Upward SW (W m^{-2})	Kipp and Zonen CG3	0.4%	
				Downward LW (W m^{-2})			
AWS_{g09}	Ablation area 2770 m a.s.l.	13 June - 4 September 2009	30 min	Aspirated air T (°C)	Vaisala HMP45C	±0.2°C	*Dumont et al.* (2012)
				Relative humidity (%)	Vaisala HMP45C	3%	
				Wind speed (m s^{-1})	Young 05103	0.3 m s^{-1}	
				and direction (degrees)	Young 05103	±3°	*Litt et al.* (2016)
				Upward SW (W m^{-2})	Kipp and Zonen CG3	0.4%	
				Downward LW (W m^{-2}) Albedo			

Table 1. AWS sensor characteristics, locations and measurement periods.

2.3.4 Adjusted SAFRAN data

SAFRAN data were compared to the AWS_m measurements over 10 years (2005-2015) and to the available AWS_g measurements. Biases were adjusted and the influences of all corrections mentioned below on the simulated SMB are discussed in section 4.3. SAFRAN and AWS_m hourly air temperatures over the ablation and accumulation seasons are well correlated (R^2 = 0.98 (summer) and 0.99 (winter), both significant at the 99% confidence level (Student's *t* test) without systematic bias). Hourly SAFRAN relative humidity is also in good agreement with the AWS_m data (R^2 = 0.74, significant at the 95% confidence level). The comparison between SAFRAN and AWS_m incoming long wave radiation indicates an overestimation of SAFRAN data for low cloudiness conditions. This can be explained by local orographic features and/or low-altitude clouds that are not considered in SAFRAN reanalysis. As proposed by Dumont *et al.* (2012), we corrected the long wave incident radiation (LW in W m^{-2}) by implementing a linear function depending on SAFRAN cloudiness (ranging from 0 to 1) (Eq. 1):

$$LW_{corrected} = LW_{SAFRAN} - (a*Cloudiness + b) \quad (1)$$

where a = -0.56 and b = 38 W m^{-2} are empirical parameters, calibrated with AWS_m measurements. This correction was calibrated over the 2005-2015 period and applied over the 1995-2015 period. Using this correction, the correlation between AWS_m incoming LW radiation and corrected LW radiation from SAFRAN increased from R^2 = 0.84 to R^2 = 0.91.

A poor correlation (R^2 = 0.25) between SAFRAN wind speed (generally considered at 2-m) and measured values at AWS_m (at ~2-m) is observed and is mainly due to an underestimation of strong winds by SAFRAN. Differences between AWS_m and SAFRAN wind speed range from 0.9 to 21 m s^{-1} with a mean value of 4.3 m s^{-1}. This underestimation is likely due to both non-consideration of katabatic wind and local effects due to orography. The wind speed measured at AWS_m (glacier foreland) were first compared to the wind measured at AWS_{g06} and AWS_{g09}. Since the correlation between the measured wind speed on the foreland and on the glacier is high (R^2=0.97), we assumed the wind speed measured at AWS_m to be representative at the glacier scale and used it to replace SAFRAN wind speed estimates in this study. However, data is limited to the 2005-2015 period. Outside this period (over 1995-2004), the SAFRAN wind speed was corrected using a quantile-mapping method (Déqué, 2007; Gobiet *et al.*, 2015). This method was chosen because it is considered to be one of the most efficient bias adjustment methods available (e.g., Gobiet *et al.*, 2015). Percentiles of the observed distribution (AWS_m measurements) and the SAFRAN distribution are calculated using every data of a given month and for each month over the 2005-2015 period. A linear method was used for mapping and extrapolated data over the minimum/maximum observed quantile were estimated with a linear function. The resulting mapping function of the quantile-quantile plot was used to adjust the SAFRAN wind speed distribution over the 1995-2004 period.

Finally, SAFRAN cumulated winter precipitation over each winter was compared to the WSMBs measured at each

accumulation measurement site. As already mentioned in previous studies (Gerbaux *et al.*, 2005; Dumont *et al.*, 2012), using SAFRAN raw data leads to a significant underestimation of the WSMB. The accumulation amount was adjusted based on the methodology developed in previous studies (Vincent, 2002; Gerbaux *et al.*, 2005; Dumont *et al.*, 2012; Réveillet *et al.*, 2017). For each winter, individual WSMB measurements were first used to compute multiplication factors for SAFRAN precipitation. The multiplication factors were then spatially interpolated over the entire glacier surface area (kriging method) to obtain an annual map of multiplicative factors. These factors were then used to correct solid and liquid precipitation. The factors varied from 1.2 to 2.1 depending on both the year and the site. Applying these factors led to an increase in WSMB ranging from 0.05 m w.e. yr^{-1} to 1.64 m w.e. yr^{-1} depending on the site (with a mean of 0.46 m w.e. yr^{-1}).

All adjustments of the raw SAFRAN data described below are summarized in Figure 2. The impact of these corrections on the simulated SMB is discussed in section 4.2.2.

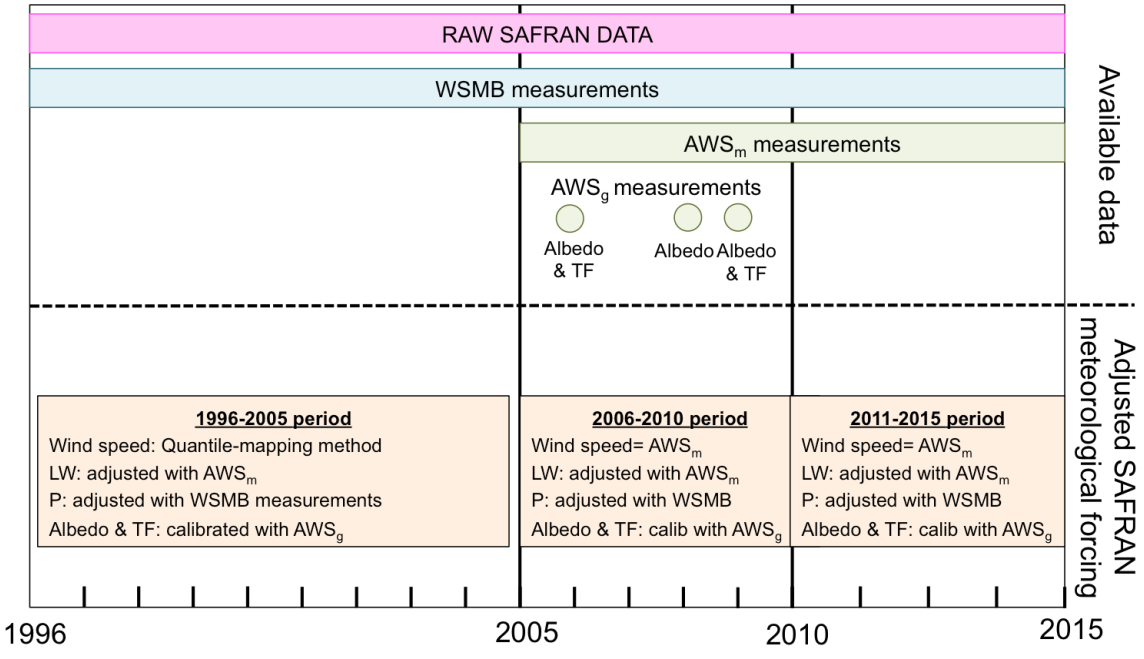

Figure 2. Summary of available meteorological data and the adjustments of the raw SAFRAN data, depending on the study period (TF = Turbulent Fluxes).

The Cryosphere Discuss., https://doi.org/10.5194/tc-2017-188
Manuscript under review for journal The Cryosphere
Discussion started: 22 September 2017

3 Methodology: model descriptions and evaluation metrics

3.1 Model descriptions

3.1.1 Crocus model

The Crocus snowpack model implemented as one of the snow scheme options of the SURFEX/ISBA land surface model (Masson *et al.*, 2013) was originally developed by Météo-France to simulate seasonal snowpack and to assist in avalanche hazard forecasting over the French mountain ranges (Brun *et al.*, 1989; Vionnet *et al.*, 2012). Crocus is a full energy balance, one-dimensional snowpack model, driven by meteorological variables including temperature, shortwave radiation, longwave radiation, specific humidity, rainfall and snowfall rates and wind speed. It simulates a layered snowpack with a Lagrangian representation, each layer being characterized by its thickness, density, temperature, liquid water content and two semi-empirical variables to describe the snow/ice microstructure. The number of numerical snow layers evolves with time to tend towards an idealized prescribed thickness profile that is appropriate for the computation of an accurate energy balance (thinner layers close to the surface) but that avoids the aggregation of snow layers with different microstructural properties. The model solves the heat diffusion equation in the snowpack at a 15-minutes time step considering the different energy fluxes between the surface and the atmosphere and between the bottom of the snowpack and the soil. Physical processes such as solar radiation absorption, liquid water percolation, snow metamorphism and settlement are also considered by the model. The snowpack model can be used on icy surfaces, considering an ice layer as a specific snow layer with a density of 917 kg m^{-3} (Gerbaux *et al.*, 2005; Lejeune *et al.*, 2007; Dumont *et al.*, 2012). The specific parameterizations used in our study (albedo and roughness length) will be described in detail below. A more general presentation of Crocus can be found in Brun *et al.* (1992) and Vionnet *et al.* (2012).

In the initial version of Crocus, solar radiation is handled in three separate spectral bands ([0.3-0.8], [0.8-1.5] and [1.5-2.8] μm), and albedo is computed for each band as a function of the snow properties: grain size, shape and age (Brun *et al.*, 1992). In this initial version, snow albedo ranges from 1 to 0.7 in the UV and visible range ([0.3-0.8] μm) and depends on the optical diameter and on the amount of light absorbing impurities, the latter being parameterized with respect to the age of snow (with a time constant of 60 days). In our study, the minimum snow albedo is fixed at 0.5 to consider older snow with higher impurity content (Cuffey and Patterson, 2010) and the time constant for the impurities parameterization is reduced to 20 days. In particular, firn albedo is considered as old snow albedo. Ice albedo is constant with time for all the considered spectral bands. Values are set to [0.23, 0.16, 0.05], based on previous studies on Saint-Sorlin Glacier (Gerbaux *et al.*, 2005; Dumont *et al.*, 2012).

In Crocus, the sensible and latent heat fluxes (respectively H and LE) are calculated using the bulk aerodynamic approach, including a stability correction (Brutsaert, 1982). The two fluxes are parameterized using an effective surface roughness length z_0 (Vionnet *et al.*, 2012), with different values for snow and ice surfaces. Note that this roughness length z_0 is considered as an effective value used in the model to fix the aerodynamic (z_m), temperature (z_t) and humidity (z_q) roughness values, following the approximation: $z_0 = z_m = 10z_t = 10z_q$. The choice of appropriate values for z_0 over ice (z_{0ice}) for Saint-

Sorlin Glacier is presented in section 4.2.3.1. As no turbulent flux measurements are available for the snow surface, the snow roughness length (z_{0snow}) is arbitrarily fixed at 0.1 mm (Gromke *et al.*, 2011).

3.1.2 Temperature-index model

The empirical model selected in this study is the ATI (Alternative Temperature-Index) model proposed by Réveillet *et al.* (2017). In this approach, the daily melt is computed as follows:

$$M = Tf_{ice\,/snow} * T + If_{ice/snow} * IPOT \quad (2)$$

where $Tf_{snow/ice}$ is the temperature factor (m w.e. d^{-1} $°C^{-1}$) which depends on the surface condition (*i.e.* ice or snow), T is the mean daily air temperature (°C), $If_{snow/ice}$ is the radiation factor (m^3 w.e. d^{-1} W^{-1}) which also depends on the surface condition (*i.e.* ice or snow) and *IPOT* is the incoming potential direct solar radiation (W m^{-2}). Melt can occur when the sum of the two terms of the equation is positive, meaning that melt can occur even if T is <0°C. In this approach, $If_{snow/ice}$ represents the energy fluxes related to solar radiation, which differ for snow and ice, but are assumed constant in time (*i.e.* no temporal change in the albedo of the snow or ice is taken into account). *Tf* represents the temperature-dependent energy fluxes such as turbulent fluxes or LW radiation. Empirical factors were calibrated with punctual SMB measurements performed on Saint-Sorlin Glacier over the period 1995-2012 (more details on the model and the calibration can be found in Réveillet *et al.*, 2017).

3.2 Evaluation metrics

3.2.1 Model evaluation method

The Crocus model was applied over the 1995-2015 period and evaluated over three distinct time periods, depending on the available AWS measurements (Figure 2): (i) a calibration period (2006-2010), over which it was possible to correct both meteorological forcing and model parameterization (albedo and roughness length) using AWS_g and AWS_m measurements, (ii) the 2011-2015 period over which it was possible to correct only meteorological forcing using AWS_m measurements, and finally (iii) the 1996-2005 period over which no corrections were possible, due to the absence of AWS measurements. Results of annual, winter and summer mass balance simulation using Crocus are presented section 4.1.1.

Crocus model simulations were then compared to those obtained from the ATI temperature-index model. The ATI model was forced with the same WSMB simulated by Crocus, to compare the ability of the two models to simulate SSMB only. Comparisons were performed over two periods: (i) the period for which AWS measurements were available (2006-2015) and (ii) the period without AWS measurements available (1996-2005).

Simulations were performed with a 200-m DEM resolution (see section 2.2.2) and grid cells corresponding to stake locations were extracted for comparison between modelled and measured SMBs. Performance was evaluated by comparing both ATI and Crocus simulations to winter, summer and annual SMB measurements, for both ablation and accumulation areas. Note that comparisons were made over the exact same period, determined by SMB measurement dates. The results are presented

section 4.1.2.

Finally, the sensitivity of ASMB to both winter and summer SMB was assessed using the Crocus model at various stakes in the ablation area. First, we considered averaged winter conditions over the accumulation period (from 1 October to 15 April) by computing the average of the 20 available winters (1996 to 2015). Then, based on this averaged winter, 20 simulations of annual SMB were performed using each of the 20 summer conditions (1996-2015).

Next, we assessed the sensitivity of annual SMB to winter SMB. We considered an averaged summer by computing the mean of the SAFRAN corrected re-analysis of the twenty summers available (1996-2015). Simulations were performed using the twenty winter conditions available. The results are presented in section 4.1.3.

3.2.2 Analysis of SMB sensitivity to Crocus parameterization

3.2.2.1 DEM

First, we investigated the effect of the spatial resolution of the DEM. For this purpose, the numerical simulations were performed with a 50-m resolution grid size, based on the 2007 DEM, and were compared with the results obtained using the same DEM with a 200-m resolution grid. Second, the impact of changes in glacier surface topography with time was evaluated by performing simulations over the 2006-2010 period using the three DEMs (1998, 2007 and 2014). To evaluate these sensitivities, SSMBs simulated by Crocus were compared to SSMB measurements at each stakes and the results are presented in section 4.2.1.

3.2.2.2 Meteorological forcing

To test the impact of the correction made on the longwave radiation, wind speed and precipitation, simulations were performed using a raw SAFRAN forcing and the adjusted SAFRAN forcing described in section 2.3.4. Evaluation involved comparing SMBs simulated by Crocus with SBMs measured at each stakes, over the 2006-2010 period. The results are presented section 4.2.2. Regarding the precipitation, two additional adjustment methods were used. The first is based on the use of a single mean correction factor, computed using all available WSMBs (over the 1996-2015 period). The second method is based on the use of a temporally averaged spatialized map of multiplicative factors based on the twenty years of available measurements (as proposed by Gerbaux *et al.*, 2005 and Dumont *et al.*, 2012).

3.2.2.3 Crocus parameters

In the Crocus version used in this study, both surface roughness and albedo were calibrated using AWS measurements. Sensitivity tests were performed by varying these variables to estimate the uncertainties when no measurements are available. The effective roughness length values were varied arbitrarily by a factor of 1 to 100 and the ice albedo of the spectral band [0.3-0.8] µm were varied from 0.16 to 0.32 (in agreement with Oerlemans *et al.*, 2009). Simulations were performed at different stakes for the 2006-2010 period. The results are presented section 4.3.3.

The Cryosphere Discuss., https://doi.org/10.5194/tc-2017-188
Manuscript under review for journal The Cryosphere
Discussion started: 22 September 2017

4. Results and discussion

4.1 Surface mass balance modelling

4.1.1 Crocus performance

The Crocus model was run over the three distinct time periods and annual and seasonal SMBs were compared to measurements (Figure 3). Correlations are significant in every case at the 95% confidence interval according to a Student's *t* test.

Performance over both the period 2006-2010 and the recent period 2011-2015 is similar. WSMB correlations for the recent period are high (Nash and Sutcliffe coefficient (NS) > 0.72, (Figures 3e and 3h), Nash and Sutcliffe (1970)). This high performance results from the use of annual multiplication factors to correct precipitation to fit with accumulation measurements. As a consequence, differences between measured and simulated WSMBs (systematically lower than 0.5 m w.e.) are due to the interpolation method and some melting events which can occur over the accumulation period. For these two periods (2006-2010 and 2011-2015), SSMB simulations were also in good agreement with measurements (NS > 0.85) in both accumulation and ablation areas (Figures 3f and 3i), indicating good performance of the model in simulating SMB changes over the ablation season. Due to both good WSMB and SSMB simulations, results at an annual scale (Figures 3d and 3g) also showed the good performance of the model (NS > 0.67).

Regarding the period 1996-2005 (Figure 3, a-b-c), while correlations between measured and simulated SMBs are significant at the 95% confidence interval according to a Student's *t* test, results indicate lower performance, especially for the simulation of the SSMBs (Figure 3c). Simulated SSMBs and annual SMBs (Figures 3a and 3c) are over-estimated for very negatives SSMBs observed in 2002/2003 in the ablation area.

4.1.2 Comparison with the temperature-index approach

Over the period 2006-2015, results indicate better performance with the Crocus model (Figures 4a and b). Indeed, the ATI model over-estimated the SSMB values greater than -2 m w.e. in particular those corresponding to the accumulation area (Figure 4b)), leading to a significant decrease in the correlations between measurements and simulations. However, when considering SSMB measurements in the ablation area only, performance is similar for the two models (NS is 0.47 for Crocus and 0.51 for the ATI model). In addition, the temporal evolution of simulated SSMBs over one hydrological year (not shown) indicates similar performance for the two models in the ablation area (maximum difference of SSMB is 0.36 m w.e. yr^{-1}). In the accumulation area and close to the equilibrium line, differences of SSMB are larger and can reach 0.84 m w.e. yr^{-1}.

Over the period 1996-2005, considering all the point data over the entire glacier, Crocus performs better than the ATI model (Figures 4c and d). Here again, SSMBs simulated with the ATI model in the accumulation area are over-estimated. On the other hand, when considering the ablation area only, results from the ATI model better fit the SSMB measurements (NS is 0.36 for Crocus and 0.59 for the ATI model). Decreasing Crocus performance over the 1996-2005 period can be explained

The Cryosphere Discuss., https://doi.org/10.5194/tc-2017-188
Manuscript under review for journal The Cryosphere
Discussion started: 22 September 2017

by the absence of AWS measurements to evaluate and validate the correction made on the wind speed and longwave forcing data.

Note that the ATI was calibrated over the period 2005-2015 and is stable over the 20 years of simulations, considering an uncertainty of 0.2 m w.e. (Réveillet *et al.*, 2017). However, stability of the parameters over a period of more than two decades cannot be guaranteed.

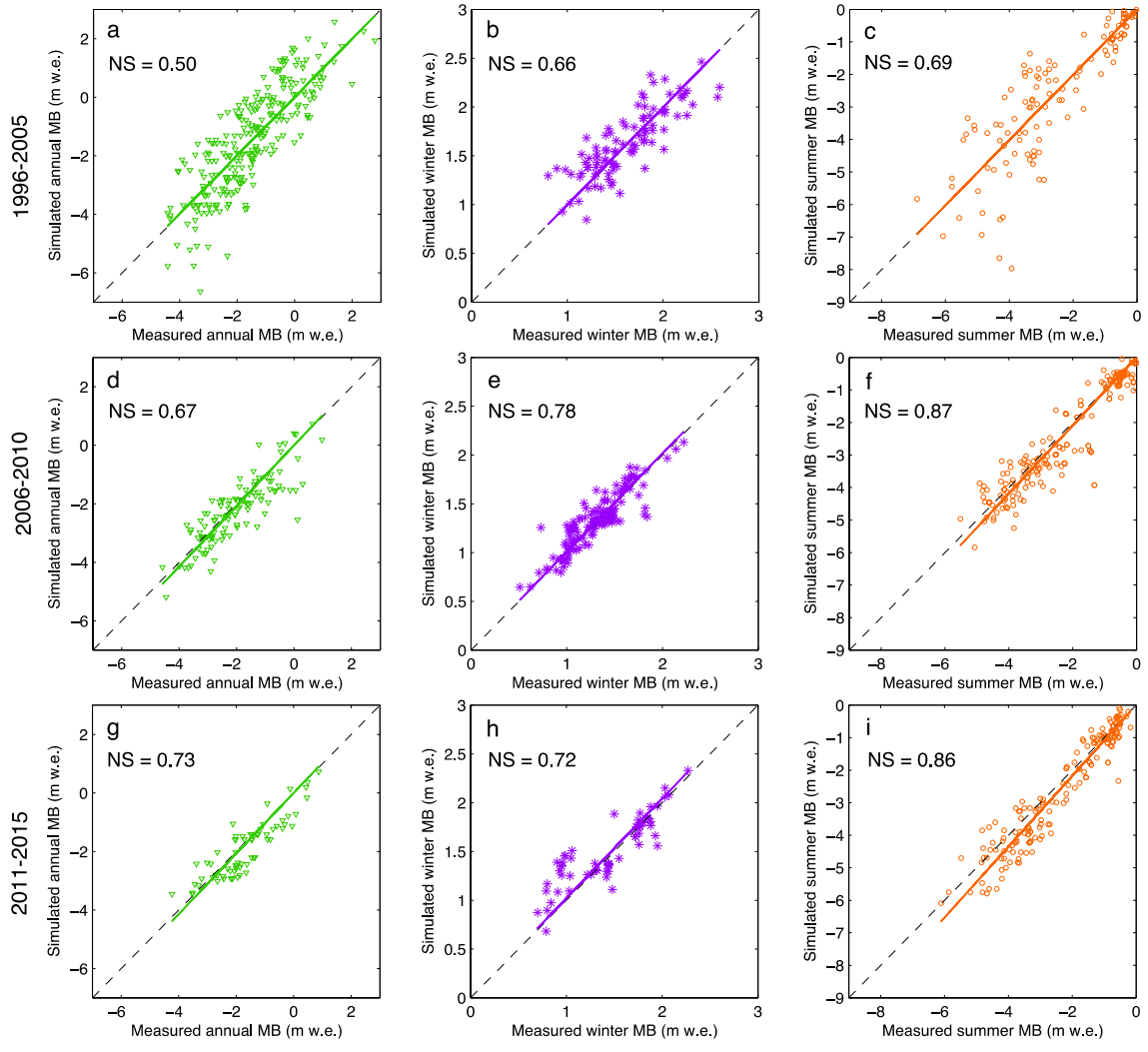

Figure 3. Comparisons between simulated and measured SMBs (m w.e.) at each measurement point over the 1996-2005 (in-situ meteorological measurements not available; a, b, c), 2006-2010 (in-situ meteorological measurements available on the moraine and on the glacier; d, e, f) and 2011-2015 (in-situ meteorological measurements available on the moraine only; g, h, i) periods. The annual (a, d, g), winter (b, e, h) and summer (c, f, i) SMBs are shown in green, purple and orange, respectively. The Nash and Sutcliffe coefficient (NS) is indicated on each graph.

The Cryosphere Discuss., https://doi.org/10.5194/tc-2017-188
Manuscript under review for journal The Cryosphere
Discussion started: 22 September 2017

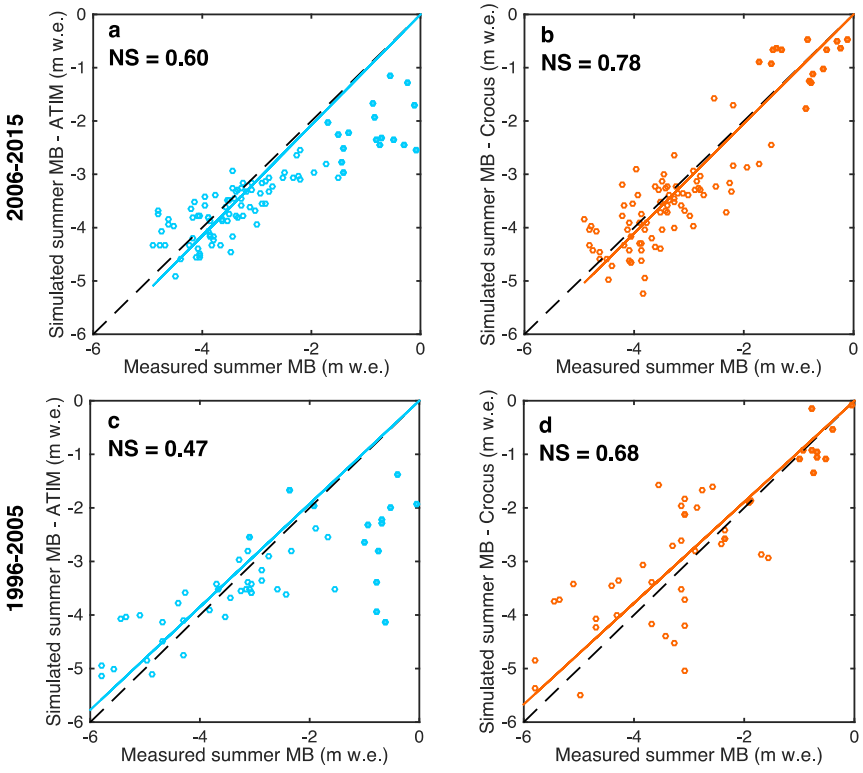

Figure 4. Correlations between simulated (blue (a-c) for the ATI model and orange (b-d) for the Crocus model) and measured SSMBs at each stake of Saint-Sorlin Glacier over the 2006-2015 period (a-b) and the 1996-2005 period (c-d). Circles represent measurements in the ablation area and solid dots represent measurements in the accumulation area.

4.1.3 Annual mass balance sensitivity to seasonal mass balance

The tests described in section 3.2.1 using the Crocus model were performed at various stakes in the ablation area. For the sake of clarity, only the results for stake #10 (located at 2760 m a.s.l.) are presented here (Figure 5), but conclusions are similar for all the stakes.

Regarding the sensitivity of annual SMB to SSMB (Figure 5a), the results show that the simulated annual SMB was the least negative with 1995 summer conditions (green curve) and the most negative with 2003 summer conditions (red line). The difference in annual SMBs between these two extreme summers was 4.1 m w.e. yr^{-1} at the end of the hydrological year.

The sensitivity of annual SMB to WSMB is illustrated by Figure 5b. Note that for the sake of clarity, only the two extreme years of the time series (2000-2001, highest WSMB (pink line) and 2008-2009, lowest WSMB (blue line)) are presented in Figure 5b. The difference between these two years on 15 April is 1.2 m w.e. Using the same summer conditions, the difference at the end of the hydrological year is 2.4 m w.e. (*i.e.* twice the difference at the end of the winter season). The

The Cryosphere Discuss., https://doi.org/10.5194/tc-2017-188
Manuscript under review for journal The Cryosphere
Discussion started: 22 September 2017

same test was performed using the extreme 2003 summer conditions instead of the mean summer conditions. In this case, the difference at the end of the hydrological year was considerably larger (3.50 m w.e., results not shown).

These results confirm that the annual SMB variability is mainly driven by the SSMB variability (*i.e.* differences are larger when we considered a mean winter and all the summer conditions than the contrary). Nevertheless, the sensitivity of the annual SMB to the WSMB is significant, in particular for extreme years.

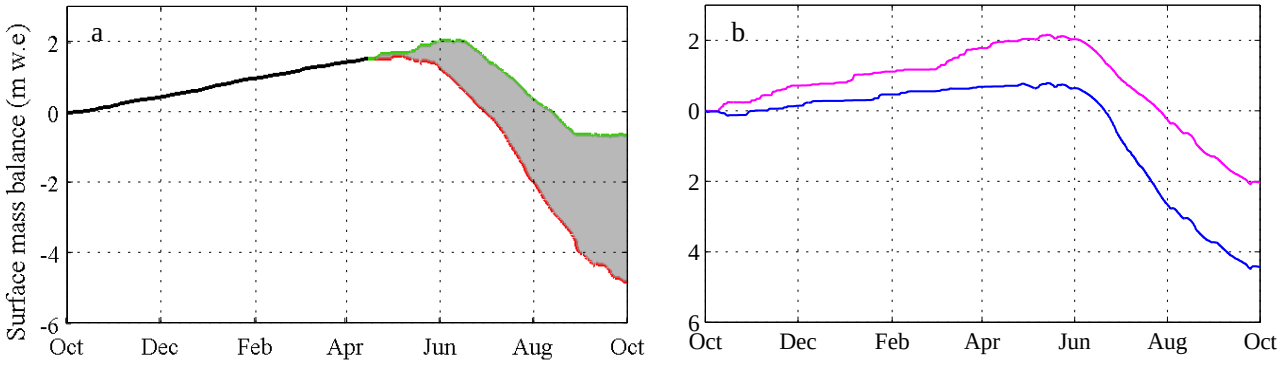

Figure 5. (a) Surface mass balance at stake #10, (2760 m a.s.l.) over one hydrological year, using averaged winter conditions and all summer conditions for the period 1995-2015. Red line represents simulation with 2003 summer conditions and the green line represents 1995 summer conditions. All the other years are included in the grey area. (b) Surface mass balance at stake #10, over one hydrological year, using averaged summer conditions (over 1995-2015), 2000-2001 winter conditions (pink) and 2008-2009 winter conditions (blue), representing the two extreme results.

4.2 Sensitivity of SMB to Crocus parameterization

4.2.1 Digital elevation model resolution and date

Regarding the effect of the spatial resolution of the DEM (*i.e.* 50-m *vs* 200-m resolution grid), changes in WSMB are negligible (NS coefficients are equal). Surprisingly, our results also indicate similar performance in simulating the SSMB when using a 50-m or 200-m resolution DEM (not shown here), even if changing the resolution impacts the calculation of slope and aspect and affects the incoming radiation computation (shadowing effect).

On the other hand, the comparison between the 1998 and 2014 DEMs shows surface elevation lowering ranging from 0 to -52 m and an average slope increase from 0 to 6°, with larger slope changes found in the ablation area. The impact of these changes was evaluated for different areas. First, correlations were computed for all the stake measurements (in the accumulation and ablation areas), then for the stakes located in the ablation area only and finally for the stakes located in the lower part of the glacier tongue (Table 2). The differences between the simulated and measured SSMBs are reported in Table

2 (correlations are not statistically different). The highest differences between simulations and measurements are obtained for the stakes located in the lower part of the glacier tongue, using 1998 and 2007 DEMs (*i.e.* where geometric changes are the greatest). Simulations performed with 1998 and 2007 DEMs led to a mean difference in simulated SSMBs of 0.19 m w.e. yr^{-1} and reached 0.64 m w.e. yr^{-1} for the lowest stakes (~15% of the SSMBs and ~20% of the ASMBs). Simulations performed with 2007 and 2014 DEMs, led to a mean difference of 0.15 w.e. yr^{-1} and a maximum of 0.47 w.e. yr^{-1} for the lowest stakes. Note that the differences in simulated SSMBs *vs.* measurements in the accumulation area are larger when considering the DEMs from 2014 and 2007 than with 1998 and 2007 DEMs and can reach 0.38 m w.e. yr^{-1} (~20% of the SSMBs and ~25% of the ASMBs). Despite changes in glacier surface topography over the entire study period, such changes only slightly affect the simulated SSMB for a limited number of individual stakes.

DEM date	*NS* (all stakes)	*NS* (stakes of the ablation area)	*NS* (stakes close to the tongue)
1998	0.87	0.41	0.79
2007	0.87	0.42	0.85
2014	0.86	0.47	0.82

Table 2. NS efficiency coefficient for simulated summer mass balances with respect to measured values over the 2006-2010 period using different 200-m resolution DEMs. The evaluation was performed using all stake measurements, only stakes located in the ablation area and stakes located in the tongue of the glacier where geometry changes are larger.

4.2.2 Meteorological inputs

An important question is whether the Crocus model forced with SAFRAN reanalysis data could be used on a large set of glaciers or over a long time period without *in-situ* meteorological measurements available to evaluate or correct the atmospheric forcing. The sensitivity of the model to the corrections made on the meteorological forcing described in section 2.3.4 and summarized in Figure 2 is presented below. Uncertainties are calculated over the 2006-2010 period, at each measurement point of the glacier.

4.2.2.1 Sensitivity to precipitation correction

SAFRAN precipitation was corrected annually using an extensive data set of WSMBs on Saint-Sorlin Glacier. Here we test different approaches to correct SAFRAN precipitation to consider the case when such extensive measurements are not available.

First, as already mentioned in previous papers (e.g., Gerbaux *et al.*, 2005; Dumont *et al.*, 2012), using raw SAFRAN precipitation leads to an underestimation of the WSMB due to the lack of observations in high altitude areas and the complexity of considering local effects such as wind transport. Using raw SAFRAN precipitation data leads to a very low NS coefficient for simulated WSMBs with respect to observed values (Table 3). This difference in terms of WSMB also

strongly impacts the performance in simulating SSMB and annual SMB (Table 3).

Second, based on the results provided by a method using a single mean correction factor over the entire glacier surface area, equal to 1.73 for Saint-Sorlin Glacier, there is a significant decrease in the correlation between measured and simulated WSMBs and lower performance in the simulation of SSMBs (Table 3).

Finally, the use of an averaged spatialized map of multiplicative factors also showed a decrease in the efficiency of both winter and summer SMB estimates (NS decreased from 0.78 to 0.15 and from 0.87 to 0.77 respectively).

These results suggest that, for Saint-Sorlin Glacier, the accuracy of the seasonal SMB computation is affected by the spatial and temporal aspects of the precipitation adjustment. This highlights the importance of considering local effects driving the spatio-temporal variability of the WSMB, such as wind transport and sublimation.

	NS for ASMB	*NS* for WSMB	*NS* for SSMB
Annual map of factors	0.67	0.78	0.87
No adjustment	-0.01	-0.03	0.23
Constant factor : 1.73	0.47	0.09	0.75
Mean factors on 1996-2015 period	0.49	0.15	0.77

Table 3. NS efficiency coefficients for simulated surface mass balances with respect to measured values over the 2006-2010 period. Simulations were performed using three different approaches to correct precipitation and were evaluated for the WSMB, SSMB and annual SMB.

4.2.2.2 Sensitivity to incoming longwave radiation

The impact of the incoming longwave radiation corrections is significant and considerably affects the simulated SSMB. A good example is the 2007-2008 hydrological year shown in Figure 6 (pink curves). Because the SAFRAN raw incoming longwave radiation is over-estimated for low cloudiness conditions (by about 30%), the correction leads to a decrease in the energy available for melt and thus a less negative SSMB. Simulations performed with and without longwave correction indicate a mean difference (computed with all available measurements over the 2006-2010 period) at the end of the season of 0.54 m w.e. yr^{-1} (with a standard deviation equal to 0.60 m w.e. yr^{-1}). Hence, not considering the incoming longwave radiation correction leads to a significant decrease in the NS coefficient (see Table 4). Note also that Sautner and Obleitner (2015) found a high sensitivity of the Crocus snowpack model to errors of incident longwave radiation over glaciers in Svalbard.

	NS for ASMB	*NS* for WSMB	*NS* for SSMB
SAFRAN with corrected data	0.67	0.78	0.87
Without LW correction	-0.02	0.67	0.65
Without Wind correction	-0.04	0.58	0.70

Table 4. NS efficient coefficients for simulated surface mass balances with respect to measured values over the 2006-2010 period. Simulations were performed using three different approaches to correct precipitation and are evaluated for the WSMB, SSMB and annual SMB.

The Cryosphere Discuss., https://doi.org/10.5194/tc-2017-188
Manuscript under review for journal The Cryosphere
Discussion started: 22 September 2017

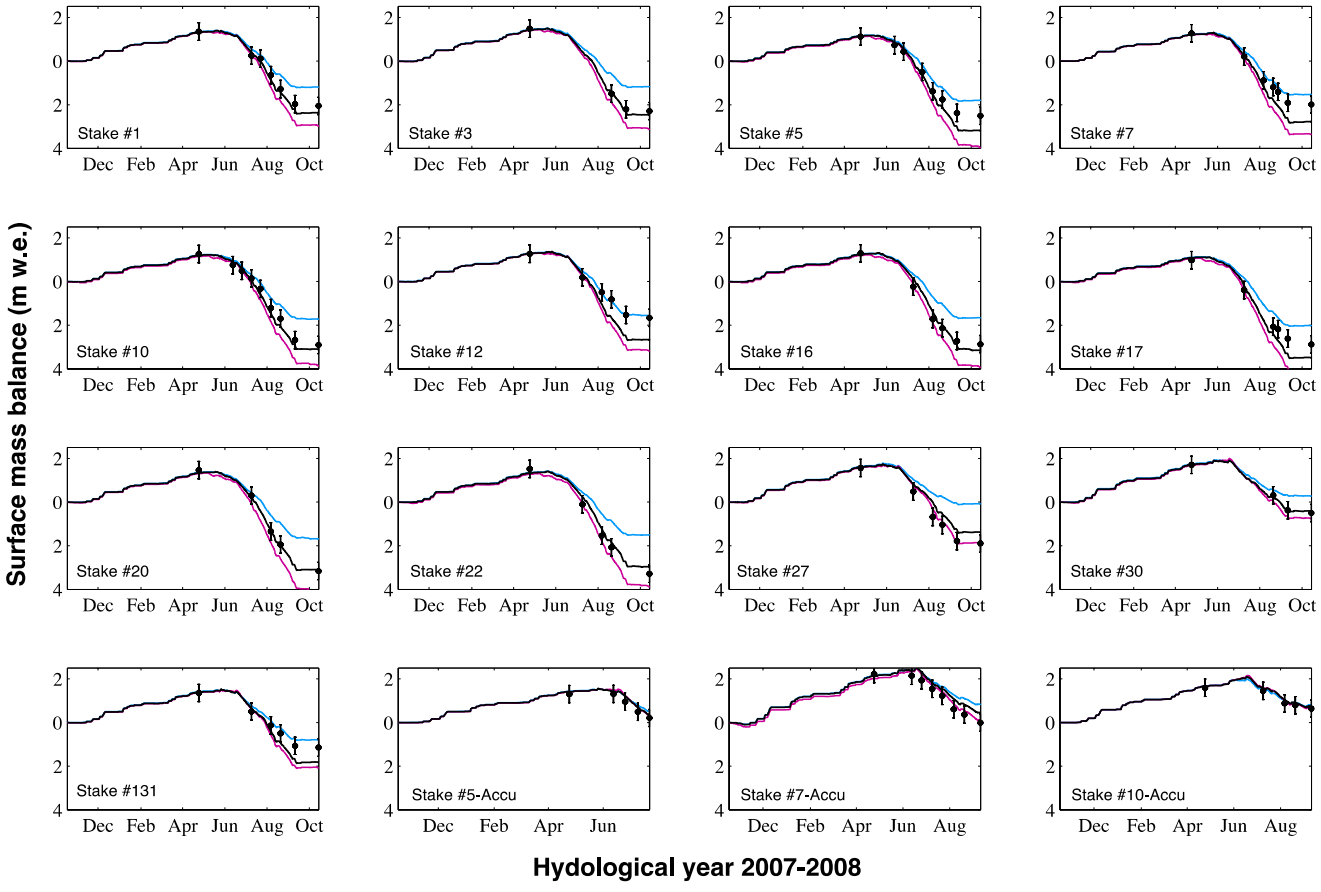

Figure 6. Surface mass balance (in m w.e.) at some selected measurement points in the accumulation (Accu) and ablation areas of Saint-Sorlin Glacier (numbers refer to the stake numbers shown in Figure 1) over the hydrological year 2007-2008 (from 17 October to 10 October). Black curves represent the simulated mass balance with corrected forcing (section 2.3.4). Pink curves are the simulations without the incoming longwave radiation correction. Blue curves are the simulations without the wind correction. Black dots represent the measurements and their uncertainties.

4.2.2.3 Sensitivity to wind speed correction

The impact of wind speed on the simulated mass balance was assessed over the period 2006-2010 using the wind speed data from AWS_m and from SAFRAN (Figure 6, blue and black curves). The mean difference at the end of the hydrological year, considering all stakes, is -0.70 m w.e. yr^{-1} (with a standard deviation equal to ±0.76 m w.e. yr^{-1}), with a maximum difference of -1.72 m w.e. yr^{-1} (Stake #16 in Figure 6). The use of uncorrected wind data significantly decreases the performance of the annual SMB simulations (the NS coefficient decreases from 0.67 to -0.04 (Table 4)).

The influence of wind speed and direction on snow accumulation variability during and after snowfall events is widely

recognized (e.g., Winstral and Marks, 2002). Our results emphasize the important role of wind speed in energy balance exchanges and its impact on the SMB (Figure 6). Indeed, wind impacts the snow surface density through snow compaction (e.g., Vionnet *et al.*, 2012) and the turbulent fluxes (e.g., Litt *et al.*, 2016). Actually each component of the turbulent fluxes (H and LE) simulated with original SAFRAN wind data is about ten times lower than those simulated with the measured wind (not shown here). Considering wind speed data from AWS_m leads to an increase in the snow density of about 50 kg m^{-3} for the upper layers of the snowpack when density is lower than 300 kg m^{-3}. Above this value, densities are similar with and without wind speed correction. The changes in snow density directly affect the thermal conductivity of the upper snow layers (Yen, 1981).

As a consequence, differences in snow density, and even more so in turbulent fluxes, due to wind speed correction have a considerable impact on surface temperature (Figure 7). Over the period 2006-2010, the mean simulated snow surface temperature increases by 3.4 °C using corrected wind speed (up to 20 °C) and the mean ice surface temperature increases by 2.7 °C (up to 10 °C), with larger differences during the night.

Simulated surface temperatures were compared to measurements. During winter, when snow depth is sufficient (~20 cm) and energy balance not affected by ground fluxes, outgoing LW measured at AWS_m can provide the snow surface temperature using the Stephan Boltzmann law (with an uncertainty of 1°C). During summer, outgoing LW measurements from AWS_{g06} were used to compare simulated and measured surface temperatures. Figure 7 illustrates the impact of the wind correction on the simulated surface temperature and the comparison with measurements in 2006. Results indicated a significant increase in correlation between measured and simulated surface temperatures when corrected wind was considered (NS increase from -3.14 to 0.28 for the summer period and from -0.30 to 0.20 for the winter period). Nevertheless, even using corrected wind speed values, simulated surface temperatures are still lower than the measurements, especially over the winter period. Note that the surface temperature also has a positive feedback on the turbulent fluxes, leading to a complex relation between these variables.

During the winter season, surface temperatures (measured or simulated) are in any case too low for melting to occur and consequently the impact of the correction of wind on the winter SMB is negligible (Figure 6). The impact of surface temperature can be first observed in spring: if surface temperature during the night is too low, the available energy during the day is used only to warm the snow layer and not for melting. A larger impact of the correction of wind on SMB can be observed over icy surfaces (from about July for ablation stakes, Figure 6), indicating the importance of having wind speed measurements to compute turbulent fluxes.

4.2.3 Sensitivity of Crocus parameters

As mentioned in the previous section, even when considering measured wind speed, a difference persists between the measured and simulated surface temperatures. Sensitivity tests were performed to better understand the processes responsible for this under-estimation of simulated surface temperatures.

The Cryosphere Discuss., https://doi.org/10.5194/tc-2017-188
Manuscript under review for journal The Cryosphere
Discussion started: 22 September 2017

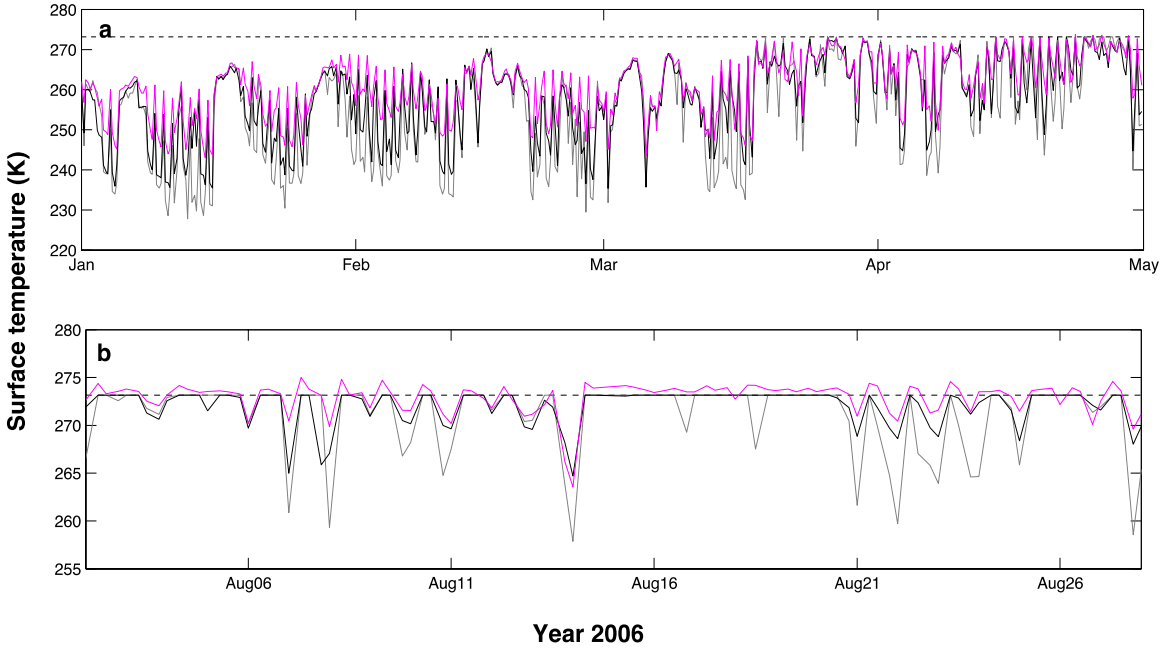

Figure 7. (a) Winter hourly surface temperature (snow surface) from January to May 2006, measured using outgoing LW radiation at AWS_m (pink) and simulated without (grey) and with (black) wind speed correction. (b) Summer hourly surface temperature measured using LWout at AWS_{g06} (pink) and simulated without (grey) and with (black) wind speed correction from 9 July to 28 August 2006.

4.2.3.1 Surface roughness length

While feedback loops exist between turbulent fluxes and surface temperature, we attempted to assess the impact of effective roughness length values (varying arbitrarily from a factor 1 to 100) on both surface temperature and summer SMB (Figure 8). Figure 8a illustrates a stronger impact for more negative SSBMs (corresponding to mainly ice ablation) than for the less negative SSMBs (corresponding to snow ablation). This is confirmed by results shown in Figures 8b and 8c. In fact, changing the roughness length considerably affects the simulated ice ablation (Figure 8b) but does not affect the simulated snow ablation (Figure 8c) and snow surface temperature (results not shown).

In this study, z_0 is calibrated to provide good agreement between the simulated and measured turbulent fluxes on the ice from 9 July to 28 August 2006 (Litt *et al.*, 2016; see section 2.3.2). For this, numerical experiments were performed using an ice roughness length z_{0ice} ranging from 10^{-5} to 0.2 m. The best simulation performed with Crocus was obtained with an ice roughness length (z_{0ice}) of 1 mm. Note that z_0 was calibrated by fitting the simulated sum of H and LE with the one calculated with the EC method. However, turbulent flux measurements are available over a short time period, only for one ablation season. As z_0 can vary considerably over time and space, and due to the strong sensitivity of the model to this parameter, having *in-situ* turbulent flux measurements over icy surfaces is very useful to properly calibrate z_{0ice}.

The Cryosphere Discuss., https://doi.org/10.5194/tc-2017-188
Manuscript under review for journal The Cryosphere
Discussion started: 22 September 2017

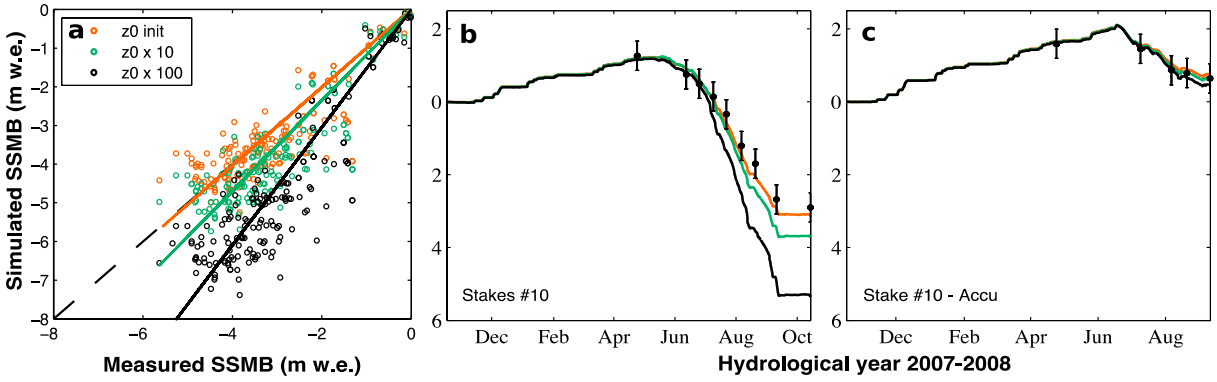

Figure 8. (a) Correlations between simulated and measured SSMBs at each measurement point over the 2006-2010 period, using different roughness lengths. Surface mass balance evolution at one stake in ablation area (b) and at one stake in accumulation area (c) over the hydrological year 2007-2008. SMB was simulated using different roughness length values for snow and ice (z_{0ice} = 1 mm and z_{0snow} = 0.1 mm (orange); z_{0ice} = 10 mm and z_{0snow} = 1 mm (red) and z_{0ice} = 100 mm and z_{0snow} = 10 mm (black)).

4.2.3.2 Ice albedo

Simulations to test Crocus parameter sensitivity to ice albedo were performed in the ablation area for the 2006-2011 period by changing the ice albedo of the spectral band [0.3-0.8] µm from 0.16 to 0.32. For the sake of clarity, Figure 9 illustrates the results for stake #10 for the hydrological year 2007-2008, but results are similar for the other stakes and over the other hydrological years. The difference in annual SMBs at the end of the hydrological year is 0.48 m w.e. yr^{-1} (17% of the ASMBs). This parameter needs to be properly calibrated with measurements to optimize model performance but does not represent the main source of uncertainty.

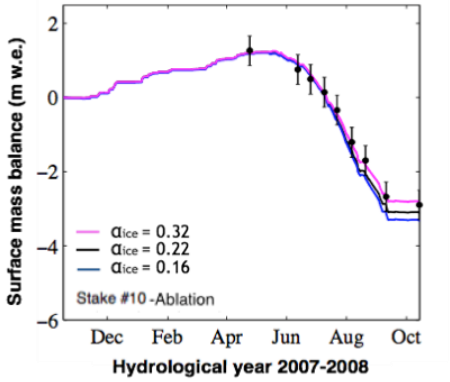

Figure 9. Surface mass balance evolution with an ice albedo calibrated at 0.16 (blue), 0.22 (black) and 0.32 (pink), at one stake in ablation area over the hydrological year 2007-2008.

4.2.3.3 Liquid water content at the surface

During melting events the simulated liquid water percolates through the snow layers when the liquid water volumetric content exceeds 5% of the pore volume (Vionnet *et al.*, 2012). For ice, the porosity is set to 0 so the liquid water immediately flows off the glacier and cannot remain at the surface. The use of such parameterization on ice is questionable as water from ice melt or from shallow snow layer melt above ice can stay at the surface.

A sensitivity test was performed, considering ice as a porous material, able to store liquid water in 10% of its total volume. Note that this sensitivity test is an over-simplistic way to consider the presence or not of water at the ice surface. As the water percolates very quickly, the test can be performed over a very short time period during summer (few days).

For summer 2006 (not shown), a significant difference in the simulations was found for the surface temperature (maximum of 20 °C difference) and surface mass balance (difference of 0.6 m w.e. after 15 days of simulation) when the possibility for water to be stored at the glacier surface was considered or not. While such test is simplistic, it indicates the significant sensitivity of the energy budget to the presence of liquid water on the ice surface. This process deserves to be properly taken into account in Crocus when using the snow model over ice surfaces, as has been done for summer SMB simulations in Greenland with other models (e.g., Gallée and Duynkerke, 1997; Lefebre, 2003; Fettweis, 2007).

5. Conclusion

This study evaluated the performance of the Crocus snowpack model, which was fed with SAFRAN reanalysis data, thereby simulating seasonal and annual SMBs of Saint-Sorlin Glacier over the last 20 years. Using meteorological forcing adjusted with *in-situ* measurements, our results showed very good performance of the model to simulate summer SMB in both accumulation and ablation areas. Performance of the model decreased for the 1996-2005 period due to the absence of *in-situ* meteorological measurements to adjust the forcing data.

According to our sensitivity study with forcing data, the results demonstrate that the Crocus model is highly sensitive to wind speed, especially for ice melt simulations. Indeed, using *in-situ* wind speed data instead of reanalysis data (where observed wind speed values larger than 10 m s^{-1} can be under-estimated by a factor 2 or 3) led to an annual mass balance decreasing more than 1.7 m w.e. yr^{-1}. Thus, without local wind speed measurements, the model's performance strongly decreases, even using wind speed data corrected via a quantile-mapping method. In addition this study confirmed the findings by Dumont *et al.* (2012) concerning the importance of correcting the incoming longwave radiation from SAFRAN.

Model calibration represents an important step to improve model performance. According to the sensitivity study of model calibration, our results highlighted the importance of calibrating the ice surface roughness using turbulent fluxes measurements. An increase in $z0_{ice}$ by a factor of 10 can have a impact of 1.5 m w.e. yr^{-1} on ice melting. Regarding the ice albedo, while having *in-situ* measurements to calibrate the model improved model performance, the sensitivity of SSMB for this variable is lower than the sensitivity to wind speed over icy surfaces (the ice melt difference reaches 0.48 m w.e yr^{-1}

when the ice albedo is divided by a factor 2). This could suggest a relatively low sensitivity of ice albedo change (due to dust or black carbon for example) for SSMB variations in the future.

Furthermore despite changes in glacier surface topography over the entire study period, our results suggested a low sensitivity to DEM resolution and geometry evolution over the 20 years analysed. Considering different DEMs over the study period did not lead to significant differences in the quantification of the glacier wide annual SMB.

Additionally, this study compared the performance of this energy balance model to an empirical approach which uses temperature and potential incoming solar radiation as inputs. Regarding simulations of SSMB for the accumulation area, our results showed better performance using the energy balance model, especially concerning simulations of snow and firn melting in the accumulation area. Regarding the ablation area of the glacier, the two approaches showed similar performance when forced with meteorological data adjusted with nearby AWS measurements. When such measurements are not available in the vicinity of the glacier, performance of the empirical model is superior although the physical processes are not properly represented. However, the temporal stability of the calibration parameters of the empirical approach need to be assessed over a longer time period before using such an approach over several decades.

While these two approaches are efficient for SSMB simulations, the WSMB simulation needs to be corrected using winter mass balance measurements. In any case, our results indicate a strong sensitivity of annual SMB to winter SMB. The understanding of the spatio-temporal variability of accumulation processes at the glacier surface needs to be more fully investigated in future work.

In conclusion, our study revealed the large role of wind speed, which controls the magnitude of turbulent fluxes, on melting. The results highlight a very serious obstacle for the future modelling of glacier mass balance, as this meteorological variable is highly unpredictable. Our results also suggested that the sensitivity of annual mass balance to accumulation and wind speed parameters is of primary significance, as compared to sensitivity to snow and ice albedo changes. However, as such data are still difficult to represent in climatic models, the accuracy of their predictions are also questionable (e.g. Terzago *et al.*, 2017). We thus suggest a careful use of the physical approach for future long-term simulations, considering the uncertainties. Although empirical approaches based on simple meteorological variables also have serious drawbacks, they could be more appropriate for simulations of glaciers in the future bearing in mind the availability of information on future meteorological variables and surface roughness.

Acknowledgements. This study was conducted in the context of the French *Service d'Observation* GLACIOCLIM (https://glacioclim.osug.fr). We would like to thank everyone who helped in collecting data during these glacier field campaigns. Most of the computations presented in this paper were performed using the Froggy platform of the CIMENT infrastructure (https://ciment.ujf-grenoble.fr), which is supported by the Rhône-Alpes region (grant CPER07_13 CIRA). The work was made possible by the contributions of Labex OSUG@2020 (Investissements d'avenir – ANR10 LABX56), the ANR program TAG 05-JCJC-0135 and the French Research Ministry. We thank Y. Durand and G. Giraud (CNRM-GAME/CEN) for providing the SAFRAN data.

References

Braithwaite, R.J. and Olesen, O.B.: Calculation of Glacier Ablation from Air Temperature, West Greenland, in: Oerlemans, J. (Ed.), Glacier Fluctuations and Climatic Change. Springer Netherlands, Dordrecht, pp. 219–233, 1989.

Brun, E., David, P., Sudul, M., Brunot, G.: A numerical model to simulate snow-cover stratigraphy for operational avalanche forecasting. J. Glaciol. 38, 13–22, 1992.

Brun, E., Martin, E., Simon, V., Gendre, C. and Coleou, C.: An energy and mass model of snow cover suitable for operational avalanche forecasting. J. Glaciol. 35, 333–342, 1989.

Brutsaert, W.: Evaporation into the Atmosphere: Theory, History and application. D. Reidel, Hingham, Mass.

Cuffey, K. and Patterson, W.S.: The physic of glaciers. Academic Press, 2010.

Cullen, N.J. and Conway, J.P.: A 22 month record of surface meteorology and energy balance from the ablation zone of Brewster Glacier, New Zealand. J. Glaciol. 61, 931–946. doi:10.3189/2015JoG15J004, 2015.

Déqué, M.: Frequency of precipitation and temperature extremes over France in an anthropogenic scenario: Model results and statistical correction according to observed values. Global and Planetary Change, 57(1), pp.16-26, 2007

Dumont, M., Durand, Y., Arnaud, Y. and Six, D.: Variational assimilation of albedo in a snowpack model and reconstruction of the spatial mass-balance distribution of an alpine glacier. J. Glaciol. 58, 151–164. doi:10.3189/2012JoG11J163, 2012.

Durand, Y., Laternser, M., Giraud, G., Etchevers, P., Lesaffre, B. and Mérindol, L.: Reanalysis of 44 Yr of Climate in the French Alps (1958–2002): Methodology, Model Validation, Climatology, and Trends for Air Temperature and Precipitation. J. Appl. Meteorol. Climatol. 48, 429–449. doi:10.1175/2008JAMC1808.1, 2009.

Fettweis, X.: Reconstruction of the 1979-2006 greenland ice sheet surface mass balanceusing the regional climate model mar, The Cryosphere, 1(1), 21–40, 2007.

Gabbi, J., Carenzo, M., Pellicciotti, F., Bauder, A. and Funk, M.: A comparison of empirical and physically based glacier surface melt models for long-term simulations of glacier response. J. Glaciol., 60, 1140–1154. doi:10.3189/2014JoG14J011, 2014

Gallée, H., and Duynkerke P. G.: Air-snow interactions and the surface energy and mass balance over the melting zone of west greenland during the greenland ice margin experiment, J. Geophys. Res., 102(D12), 13,813–13,824, doi :10.1029/96JD03358, 1997

Gerbaux, M., Genthon, C., Etchevers, P., Vincent, C. and Dedieu, J.P.: Surface mass balance of glaciers in the French Alps: distributed modeling and sensitivity to climate change. J. Glaciol. 51, 561–572. doi:10.3189/172756505781829133, 2005.

Gobiet, A., Suklitsch, M. and Heinrich G.: The effect of empirical-statistical correction of intensity-dependent model errors on the temperature climate change signal, Hydrology and Earth System Sciences, 19(10), 4055, doi :10.5194/hess-19-4055-2015, 2015

Gromke, C., Manes, C., Walter, B., Lehning, M. and Guala, M.: Aerodynamic Roughness Length of Fresh Snow. Bound.-

Layer Meteorol. 141, 21–34. doi:10.1007/s10546-011-9623-3, 2011.

Hock, R.: Temperature index melt modelling in mountain areas. J. Hydrol. 282, 104–115. doi:10.1016/S0022-1694(03)00257-9, 2003.

IPCC, Climate Change 2013: The Physical Science Basis, Contribution of Working Group I to the Fifth Assessment. Report of the Intergovernmental Panel on Climate Change, edited by: Stocker TF, Qin D, Plattner GK, Tignor M, Allen SK, Boschung J, Nauels A, Xia Y, Bex V, and Midgley PM, Cambridge University Press, Cambridge, UK and New York, NY, USA, 2013.

Lafaysse, M., Hingray, B., Etchevers, P., Martin, E. and Obled, C.: Influence of spatial discretization, underground water storage and glacier melt on a physically-based hydrological model of the Upper Durance River basin. J. Hydrol. 403, 116–129. doi:10.1016/j.jhydrol.2011.03.046, 2011.

Lefebre, F.: Modeling of snow and ice melt at ETH Camp (West Greenland): A study of surface albedo. J. Geophys. Res. 108. doi:10.1029/2001JD001160, 2003.

Lehning, M., Bartelt, P., Brown, B., Russi, T., Stöckli, U. and Zimmerli, M.: Snowpack model calculations for avalanche warning based upon a new network of weather and snow stations. Cold Reg. Sci. Technol. 30, 145–157. doi:10.1016/S0165-232X(99)00022-1, 1999.

Lejeune, Y., Bouilloud, L., Etchevers, P., Wagnon, P., Chevallier, P., Sicart, J.E., Martin, E., and Habets, F.: Melting of Snow Cover in a Tropical Mountain Environment in Bolivia : Processes and Modeling, J. of Hydrometeorology, 8(4), 922–937, doi :10.1175/JHM590.1, 2007.

Lejeune, Y., Bertrand, J.M., Wagnon, P. and Morin, S.:, A physically based model of the year-round surface energy and mass balance of debris-covered glaciers. J. Glaciol., 59(214), 327-344, 2013

Litt, M., Sicart, J.E., Six, D., Wagnon, P. and Helgason, W.D.: Surface-layer turbulence, energy-balance and links to atmospheric circulations over a mountain glacier in the French Alps. Cryosphere Discuss. 1–24. doi:10.5194/tc-2016-93, 2016

MacDougall, A. H., and Flowers G. E.: Spatial and Temporal Transferability of a Distributed Energy-Balance Glacier Melt Model, J. of Climate, 24(5), 1480–1498, doi:10.1175/2010JCLI3821.1, 2011.

Masson, V., Le Moigne, P., Martin, E., Faroux, S., Alias, A., Alkama, R., Belamari, S., Barbu, A., Boone, A., Bouyssel, F., Brousseau, P., Brun, E., Calvet, J.-C., Carrer, D., Decharme, B., Delire, C., Donier, S., Essaouini, K., Gibelin, A.-L., Giordani, H., Habets, F., Jidane, M., Kerdraon, G., Kourzeneva, E., Lafaysse, M., Lafont, S., Lebeaupin Brossier, C., Lemonsu, A., Mahfouf, J.-F., Marguinaud, P., Mokhtari, M., Morin, S., Pigeon, G., Salgado, R., Seity, Y., Taillefer, F., Tanguy, G., Tulet, P., Vincendon, B., Vionnet, V. and Voldoire, A.: The SURFEXv7.2 land and ocean surface platform for coupled or offline simulation of earth surface variables and fluxes. Geosci. Model Dev. 6, 929–960. doi:10.5194/gmd-6-929-2013, 2013.

Mölg, T. and Kaser, G.: A new approach to resolving climate-cryosphere relations: Downscaling climate dynamics to glacier-scale mass and energy balance without statistical scale linking. J. Geophys. Res. 116.

doi:10.1029/2011JD015669, 2011.

Nash, J.E., and Sutcliffe, J.V.: River flow forecasting through conceptual models part I - A discussion of principles. J. Hydrol. 10, 282–290. doi:10.1016/0022-1694(70)90255-6, 1970.

Obleitner, F., and Lehning M.: Measurement and simulation of snow and superimposed ice at the Kongsvegen glacier, Svalbard (Spitzbergen), J. Geophys. Res., 109, D04106, doi:10.1029/2003JD003945, 2004.

Oerlemans, J., Giesen, R.H. and Van Den Broeke, M.R.: Retreating alpine glaciers: increased melt rates due to accumulation of dust (Vadret da Morteratsch, Switzerland). J. Glaciol. 55, 729–736. doi:10.3189/002214309789470969, 2009.

Oerlemans, J. and Klok, E.J.: Energy Balance of a Glacier Surface: Analysis of Automatic Weather Station Data from the Morteratschgletscher, Switzerland. Arct. Antarct. Alp. Res. 34, 477. doi:10.2307/1552206, 2002.

Pellicciotti, F., Brock, B., Strasser, U., Burlando, P., Funk, M. and Corripio, J.: An enhanced temperature-index glacier melt model including the shortwave radiation balance: development and testing for Haut Glacier d'Arolla, Switzerland. J. Glaciol. 51, 573–587. doi:10.3189/172756505781829124, 2005.

Rabatel, A., Dedieu, J.P. and Vincent, C.: Spatio-temporal changes in glacier-wide mass balance quantified by optical remote sensing on 30 glaciers in the French Alps for the period 1983–2014. J. Glaciol. 1–14. doi:10.1017/jog.2016.113, 2016.

Réveillet, M., Vincent, C., Six, D. and Rabatel, A.: Which empirical model is best suited to simulate glacier mass balances? J. Glaciol. 1–16. doi:10.1017/jog.2016.110, 2017.

Senese, A., Diolaiuti, G., Mihalcea, C. and Smiraglia, C.: Energy and Mass Balance of Forni Glacier (Stelvio National Park, Italian Alps) from a Four-Year Meteorological Data Record. Arct. Antarct. Alp. Res. 44, 122–134. doi:10.1657/1938-4246-44.1.122, 2012.

Sauter, T., and Obleitner, F.: Assessing the uncertainty of glacier mass-balance simulations in the European Arctic based on variance decomposition, Geosci. Model Dev., 8, 3911–3928, doi:10.5194/gmd-8-3911-2015, 2015

Sicart, J.E., Hock, R., Six, D., 2008. Glacier melt, air temperature, and energy balance in different climates: The Bolivian Tropics, the French Alps, and northern Sweden. J. Geophys. Res. 113. doi:10.1029/2008JD010406

Sicart, J. E., Hock, R., Ribstein, P., Litt, M. and Ramirez, E.: Analysis of seasonal variations in mass balance and meltwater discharge of the tropical Zongo Glacier by application of a distributed energy balance model, Journal of Geophysical Research, 116(D13), doi :10.1029/ 2010JD015105, 2011

Six, D. and Vincent, C.: Sensitivity of mass balance and equilibrium-line altitude to climate change in the French Alps. J. Glaciol. 60, 867–878. doi:10.3189/2014JoG14J014, 2014

Six, D., Wagnon, P., Sicart, J.E. and Vincent, C.: Meteorological controls on snow and ice ablation for two contrasting months on Glacier de Saint-Sorlin, France. Ann. Glaciol. 50, 66–72. doi:10.3189/172756409787769537, 2009

Terzago, S., Von Hardenberg, J., Palazzi, E. and Provenzale A.: Snow water equivalent in the Alps as seen by gridded data sets, CMIP5 and CORDEX climate models, The Cryosphere, 11, 1625-1645, https://doi.org/10.5194/tc-11-1625-2017, 2017

Thibert, E., Blanc, R., Vincent, C. and Eckert, N.: Instruments and Methods
Glaciological and volumetric mass-balance measurements: error analysis over 51 years for Glacier de Sarennes, French Alps. J. Glaciol. 54, 522–532. doi:10.3189/002214308785837093, 2008.

Tribbeck, M.J., Gurney, R.J., Morris, E.M. and Pearson, D.W.C.: A new Snow-SVAT to simulate the accumulation and ablation of seasonal snow cover beneath a forest canopy. J. Glaciol. 50, 171–182. doi:10.3189/172756504781830187, 2004.

Vincent, C.: Influence of climate change over the 20th Century on four French glacier SMBs. J. Geophys. Res., 107, 4–12 (doi: 200210.1029/2001JD000832), 2002

Vionnet, V., Brun, E., Morin, S., Boone, A., Faroux, S., Le Moigne, P., Martin, E. and Willemet, J.M.: The detailed snowpack scheme Crocus and its implementation in SURFEX v7.2. Geosci. Model Dev. 5, 773–791. doi:10.5194/gmd-5-773-2012, 2012

Winstral, A. and Marks, D.: Simulating wind fields and snow redistribution using terrain-based parameters to model snow accumulation and melt over a semi-arid mountain catchment. Hydrol. Process. 16, 3585–3603. doi:10.1002/hyp.1238, 2002.

Yen,Y.C.: Review of thermal properties of snow, ice and sea ice, Tech. rep., DTIC Document, 1981.